Morphological Control of Calcium Oxalate Dihydrate by a Double-Hydrophilic Block Copolymer

Dongbai Zhang, Limin Qi,* Jiming Ma, and Humin Cheng

College of Chemistry, Peking University, Beijing 100871, People's Republic of China

Received August 22, 2001. Revised Manuscript Received April 19, 2002

The crystallization of calcium oxalate in aqueous solutions of a double-hydrophilic block copolymer poly(ethyleneglycol)-*block*-poly(methacrylic acid) (PEG-*b*-PMAA) has been investigated, focusing on morphological control of the calcium oxalate dihydrate (COD) crystals. It has been shown that with increasing polymer concentration, the morphology of the obtained COD crystals gradually changed from tetragonal bipyramids dominated by the {101} faces to rodlike tetragonal prisms dominated by the {100} faces, which is a morphology adopted by some plant COD crystals but not obtained in vitro previously. The concentration of calcium oxalate and the $[Ca^{2+}]/[C_2O_4^{2-}]$ ratio were also found to show considerable effects on the morphology of the obtained COD crystals. Seed growth experiments further demonstrated the drastic effect of the polymer on the COD crystal morphology. This effect was preliminarily discussed in terms of possible structural correlation between the short PMAA chain of the polymer and the COD {100} planes.

Introduction

The synthesis of inorganic materials of specific size and morphology is a key aspect in the development of new materials in fields as diverse as catalysis, medicine, electronics, ceramics, pigments, and cosmetics.[1−5] Compared with size control, morphology control is more demanding to achieve by means of classical procedures of colloid chemistry.[6] Biological systems, on the other hand, use biomacromolecules that function variously as nucleators, cooperative modifiers, and matrixes or molds to exert exquisite control over the processes of biomineralization. The resulting biominerals (e.g., shells, bones, and teeth) are distinguished by a complexity of form in association with common functions.[7−11] The strategy in which organic additives and/or templates are used to control the nucleation, growth, and alignment of inorganic particles has been universally applied for the biomimetic synthesis of inorganic materials with unusual and complex form.[12,13]

Specifically, many efforts have been devoted to morphological control of inorganic crystals by using soluble organic additives as crystal growth inhibitors or modifiers. For instance, isolated intracrystalline biomacromolecules[14−17] and a designed peptide[18] have shown distinct control of the morphology of calcite $CaCO_3$ crystals. In addition, normal low-molecular-weight or macromolecular organic additives have been shown to exert significant morphological influence on the crystallization of various crystals including $BaSO_4$,[19−21] $CaCO_3$,[22−25] and $CaHPO_4 \cdot 2H_2O$.[26] Recently, a new class of functional polymers, the so-called double-hydrophilic block copolymers,[27] was developed as novel crystal growth modifiers for the control of inorganic crystallization. These polymers consist of one hydrophilic block designed to interact strongly with the appropriate inorganic minerals and surfaces and another hydrophilic block that does not interact strongly with the inorganic

* To whom correspondence should be addressed. E-mail: liminqi@chem.pku.edu.cn.

(1) Mann, S.; Ozin, G. A. *Nature* **1996**, *382*, 313.
(2) Ahmadi, T. S.; Wang, Z. L.; Green, T. C.; Henglein, A.; El-Sayed, M. A. *Science* **1996**, *272*, 1924.
(3) Peng, X.; Manna, L.; Yang, W.; Wickham, J.; Scher, E.; Kadavanich, A.; Alivisatos, A. P. *Nature* **2000**, *404*, 59.
(4) Matijevic, E. *Curr. Opin. Colloid Interface Sci.* **1996**, *1*, 176.
(5) Adair, J. H.; Suvaci, E. *Curr. Opin. Colloid Interface Sci.* **2000**, *5*, 160.
(6) Matijevic, E. *Chem. Mater.* **1993**, *5*, 412.
(7) Mann, S., Webb, J., Williams, R. J. P., Eds.; *Biomineralization, Chemical and Biochemical Perspectives*; VCH: Weinheim, 1989.
(8) Mann, S. *Nature* **1993**, *365*, 499.
(9) Addadi, L.; Weiner, S. *Angew. Chem., Int. Ed. Engl.* **1992**, *31*, 153.
(10) Weiner, S.; Addadi, L. *J. Mater. Chem.* **1997**, *7*, 689.
(11) Fritz, M.; Morse, D. E. *Curr. Opin. Colloid Interface Sci.* **1998**, *3*, 55.
(12) Mann, S. *Biomimetic Materials Chemistry*; VCH: Weinheim, 1995.
(13) Mann, S. *Angew. Chem., Int. Ed.* **2000**, *39*, 3392.

(14) Berman, A.; Addadi, L.; Weiner, S. *Nature* **1988**, *331*, 546.
(15) Albeck, S.; Aizenberg, J.; Addadi, L.; Weiner, S. *J. Am. Chem. Soc.* **1993**, *115*, 11691.
(16) Albeck, S.; Weiner, S.; Addadi, L. *Chem. Eur. J.* **1996**, *2*, 278.
(17) Aizenberg, J.; Hanson, J.; Koetzle, T. F.; Weiner, S.; Addadi, L. *J. Am. Chem. Soc.* **1997**, *119*, 881.
(18) DeOliveira, D. B.; Laursen, R. A. *J. Am. Chem. Soc.* **1997**, *119*, 10627.
(19) Davey, R. J.; Black, S. N.; Bromley, L. A.; Cotter, D.; Dobbs, B.; Rout, J. E. *Nature* **1991**, *353*, 549.
(20) Bromley, L. A.; Cottier, D.; Davey, R. J.; Dobbs, B.; Smith, S.; Heywood, B. R. *Langmuir* **1993**, *9*, 3594.
(21) Coveney, P. V.; Davey, R.; Griffin, J. L. W.; He, Y.; Hamlin, J. D.; Stackhouse, S.; Whiting, A. *J. Am. Chem. Soc.* **2000**, *122*, 11557.
(22) Mann, S.; Didymus, J. M.; Sanderson, N. P.; Heywood, B. R.; Samper, E. J. A. *J. Chem. Soc., Faraday Trans.* **1990**, *86*, 1873.
(23) Didymus, J. M.; Oliver, P.; Mann, S.; DeVries, A. L.; Hauschka, P. V.; West broek, P. *J. Chem. Soc., Faraday Trans.* **1993**, *89*, 2891.
(24) Titiloye, J. O.; Parker, S. C.; Mann, S. *J. Cryst. Growth* **1993**, *131*, 533.
(25) Gower, L. A.; Tirrell, D. A. *J. Cryst. Growth* **1998**, *191*, 153.
(26) Sikiric, M.; Babic-Ivancic, V.; Milat, O.; Sarig, S.; Furedi-Milhofer, H. *Langmuir* **2000**, *16*, 9261.
(27) A recent review: Cölfen H. *Macromol. Rapid Commun.* **2001**, *22*, 219.

minerals or precursors and mainly promotes solubilization in water. Owing to the separation of the binding and the solvating moieties, these copolymers turned out to be extraordinarily effective in morphological control of inorganic crystals such as $BaSO_4$,[28,29] $CaCO_3$,[30−32] calcium phosphate,[33] and zinc oxide.[34] However, the great potential of this kind of polymer as additives or habit modifiers for morphological control of many other crystals has yet to be explored.

There has been considerable interest in the crystallization of calcium oxalate,[35] which is the most commonly formed biomineral in higher plants[36−38] and the primary mineral constituent in most human kidney stones.[39] Calcium oxalate presents three degrees of hydration: the thermodynamically stable monohydrate (COM, whewellite) and the metastable dihydrate (COD, weddellite) and trihydrate (COT).[40] Monoclinic COM and tetragonal COD are the most common phytocrystals and are among the main constituents of kidney stones whereas triclinic COT was rarely found in kidney stones. Some studies have focused on developing an understanding of the interactions between calcium oxalate crystals and organic templates and/or additives. For example, Langmuir monolayers,[41−43] membrane vesicles,[44] and phospholipid micelles[45] have been used for the direct crystallization of calcium oxalate. The morphological and phase changes of calcium oxalate crystals grown in the presence of surfactants,[46,47] carboxylic acids,[48] anionic polyelectrolytes,[49] and crystal-associated macromolecules[50] have also been investigated. However, morphological control of calcium oxalate crystals in vitro has been achieved to a very limited extent so far compared with the unusual morphologies adopted by plant calcium oxalate crystals. Moreover, the

mechanisms of macromolecular additive−inorganic crystal interactions are still poorly understood.

In the present work, we explored the morphological control of calcium oxalate dihydrate (COD) in the presence of a double-hydrophilic block copolymer, PEG-*b*-PMAA, to provide insights into the specific function of macromolecules in the morphological control of plant COD crystals. It was observed that the presence of PEG-*b*-PMAA generally favors the morphological transition of COD crystals from tetragonal bipyramids dominated by the {101} faces to elongated tetragonal prisms dominated by the {100} faces. The mechanism of polymer−COD crystal interaction was discussed by considering the structural fit between the polymer and the (100) face of COD crystals.

Experimental Section

Materials. A commercial block copolymer, poly(ethylene-glycol)-*block*- poly(methacrylic acid) (PEG-*b*-PMAA, PEG = 3000 g/mol, PMAA = 700 g/mol), which consists of an anionic PMAA block interacting strongly with inorganic minerals and a nonionic PEG block mainly promoting solubilization,[28] was obtained from Th. Goldschmidt AG, Essen, Germany. The copolymer was purified by exhaustive dialysis before it was used in the crystallization experiments. All the other chemicals used were of analytical grade and the water used was deionized.

Crystallization Experiments. The crystallization of calcium oxalate was conducted at room temperature ($\approx$22 °C) following the reported procedure for the crystallization of calcium carbonate.[32] A 0.1 M aqueous $Na_2C_2O_4$ solution and a 0.1 M aqueous $CaCl_2$ solution were first prepared as stock solutions. In a typical synthesis, a solution of $Na_2C_2O_4$ (0.1 M, 0.2 mL) was injected into an aqueous solution of PEG-*b*-PMAA (0.2 g L^{-1}, 20 mL). After the pH of the solution was adjusted to pH 10 by using HCl or NaOH, a solution of $CaCl_2$ (0.1 M, 0.2 mL) was added under vigorous stirring, giving a final CaC_2O_4 concentration of 1 mM. The stirring was maintained for 1 min and then the solution was covered and allowed to stand in a static condition for 24 h before the product was collected for characterization. In the experiments, the concentration of PEG-*b*-PMAA was varied from 0.2 to 2 g L^{-1}, the final concentration of CaC_2O_4 was varied from 0.5 to 4 mM, and the molar ratio $[Ca^{2+}]/[C_2O_4{}^{2-}]$ was varied from 1/2 to 2. For comparison purpose, the crystallization of strontium oxalate (SrC_2O_4) in the presence of PEG-*b*-PMAA was also carried out by a procedure similar to that for calcium oxalate.

To clearly show the effect of PEG-*b*-PMAA on the growth of CaC_2O_4 crystals, seed growth experiments were carried out. First, seed crystals were synthesized as described above under selected conditions, which were then separated by filtration and washed with water. A suitable amount of the obtained seed crystals were added to a solution of PEG-*b*-PMAA, which was followed by a normal procedure for the crystallization of CaC_2O_4 as described above.

Crystal Characterization. The resulting CaC_2O_4 or SrC_2O_4 precipitates were characterized by scanning electron microscopy (SEM) on an AMARY 1910FE microscope operated at 20 kV. Powder X-ray diffraction (XRD) patterns were recorded on a Rigaku Dmax-2000 diffractometer with Cu Kα radiation. Samples for XRD measurements were prepared by placing several drops of the suspension on a glass slide and removing the supernatant with filter paper. The remaining crystals were washed by placing a drop of deionized water and removing the excess water with filter paper. After drying at room temperature, the glass slide carrying the crystals was fixed to a specimen holder for XRD measurements.

Results

Effect of the Polymer Concentration. In the control system where the CaC_2O_4 concentration was 1

(28) Qi, L.; Cölfen, H.; Antonietti, M. *Angew. Chem., Int. Ed.* **2000**, *39*, 604.
(29) Qi, L.; Cölfen, H.; Antonietti, M. *Chem. Mater.* **2000**, *12*, 2392.
(30) Marentette, J. M.; Norwig, J.; Stockelmann, E.; Meyer, W. H.; Wegner, G. *Adv. Mater.* **1997**, *9*, 647.
(31) Cölfen, H.; Antonietti, M. *Langmuir* **1998**, *14*, 582.
(32) Cölfen, H.; Qi, L. *Chem. Eur. J.* **2001**, *7*, 106.
(33) Antonietti, M.; Breulmann, M.; Göltner, C. G.; Cölfen, H.; Wong, K. K.; Walsh, D.; Mann, S. *Chem. Eur. J.* **1998**, *4*, 2493.
(34) Öner, M.; Norwig, J.; Meyer, W. H.; Wegner, G. *Chem. Mater.* **1998**, *10*, 460.
(35) Lochhead, M. J.; Touryan, L.; Vogel, V. *J. Phys. Chem. B* **1999**, *103*, 3411.
(36) Webb, M. A. *Plant Cell* **1999**, *11*, 751.
(37) Pennisi, S. V.; McConnell, D. B.; Gower, L. B.; Kane, M. E.; Lucansky, T. *New Phytol.* **2001**, *149*, 209.
(38) Pennisi, S. V.; McConnell, D. B.; Gower, L. B.; Kane, M. E.; Lucansky, T. *New Phytol.* **2001**, *150*, 111.
(39) Grases, F.; Costa-Bauza, A.; Garcia-Ferragut, L. *Adv. Colloid Interface Sci.* **1998**, *74*, 169.
(40) Millan, A. *Cryst. Growth Design* **2001**, *1*, 245.
(41) Lochhead, M. J.; Letellier, S. R.; Vogel, V. *J. Phys. Chem. B* **1997**, *101*, 10821.
(42) Letellier, S. R.; Lochhead, M. J.; Campbell, A. A.; Vogel, V. *Biochim. Biophys. Acta-Gen. Subjects* **1998**, *1380*, 31.
(43) Backov, R.; Lee, C. M.; Khan, S. R.; Mingotaud, C.; Fanucci, G. E.; Talham, D. R. *Langmuir* **2000**, *16*, 6013.
(44) Khan, S. R.; Whalen, P. O.; Glenton, P. A. *J. Cryst. Growth* **1993**, *134*, 211.
(45) Brown, C. M.; Novin, F.; Purich, D. L. *J. Cryst. Growth* **1994**, *135*, 523.
(46) Skrtic, D.; Filipovic-Vincekovic, N.; Furedi-Milhofer, H. *J. Cryst. Growth* **1991**, *114*, 118.
(47) Tunik, L.; Addadi, L.; Garti, N.; Furedi-Milhofer, H. *J. Cryst. Growth* **1996**, *167*, 748.
(48) Cody, A. M.; Cody, R. D. *J. Cryst. Growth* **1994**, *135*, 235.
(49) Manne, J. S.; Biala, N.; Smith, A. D.; Gryte, C. C. *J. Cryst. Growth* **1990**, *100*, 627.
(50) Bouropoulos, N.; Weiner, S.; Addadi, L. *Chem. Eur. J.* **2001**, *7*, 1881.
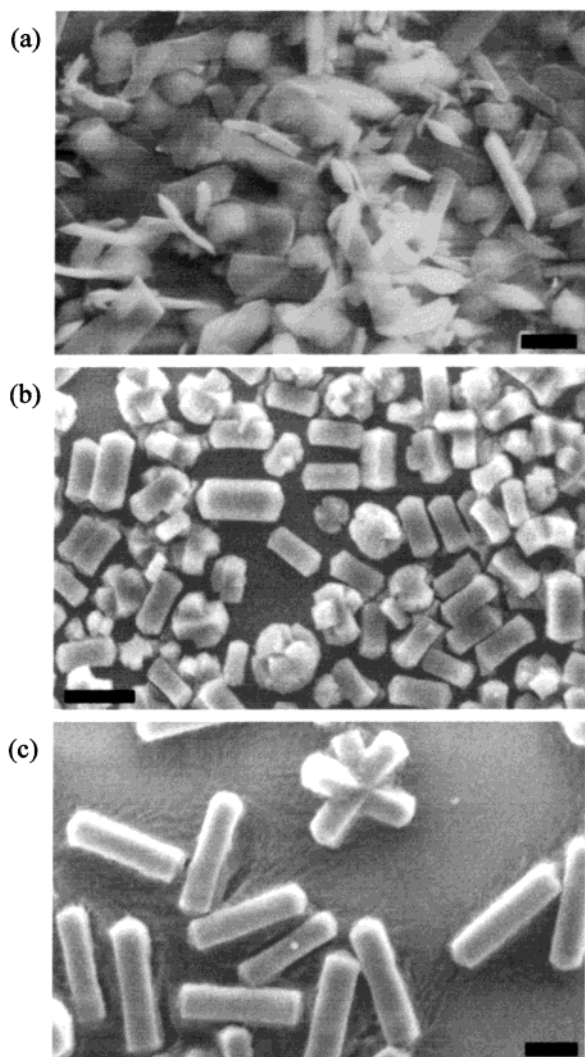
Figure 1. SEM micrographs of calcium oxalate crystals obtained in the absence (a) and the presence (b, c) of PEG-*b*-PMAA. [polymer]: (a) 0, (b) 0.2, and (c) 2 g L^{-1}; [CaC$_2$O$_4$] = 1 mM. Scale bars: (a) 5, (b) 1, and (c) 1 μm.

mM and no additives were present, a large amount of platelike crystals were obtained along with a small amount of tetragonal bipyramidal crystals about 4 μm in side length (Figure 1a). The former morphology suggested the trihydrate phase of calcium oxalate (COT)[51] whereas the latter was typical for the dihydrate phase (COD).[52] This is consistent with the corresponding XRD results shown in Figure 2a, which suggests that the obtained crystals consisted of a predominant COT phase and a minor COD phase. Considering the present high supersaturation condition, the appearance of mixed COT and COD phases would be in agreement with the argument that because COT and COD are thermodynamically unstable with respect to the monohydrate phase (COM), they have higher solubility, thereby making them kinetically favored phases.[53]

When 0.2 g L^{-1} of PEG-*b*-PMAA was present, a distinct morphological and phase change of calcium oxalate crystals occurred. As shown in Figure 1b, the

(51) Heijnen, W. M. M. *J. Cryst. Growth* **1982**, *57*, 216.
(52) Heijnen, W. M. M.; van Duijneveldt, F. B. *J. Cryst. Growth* **1984**, *67*, 324.
(53) Bretherton, T.; Rodgers, A. *J. Cryst. Growth* **1998**, *192*, 448.
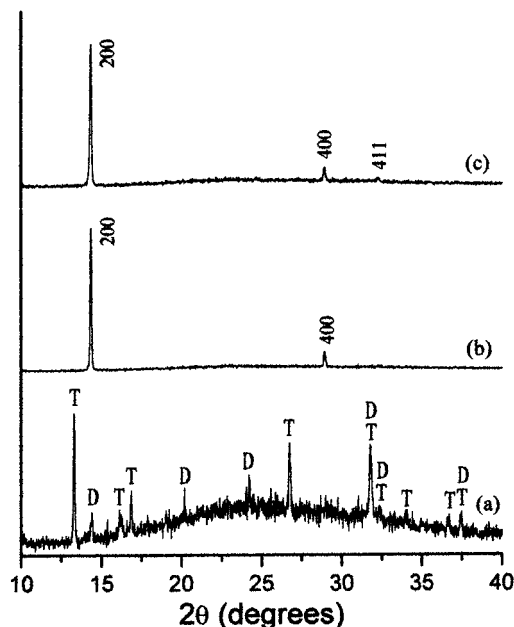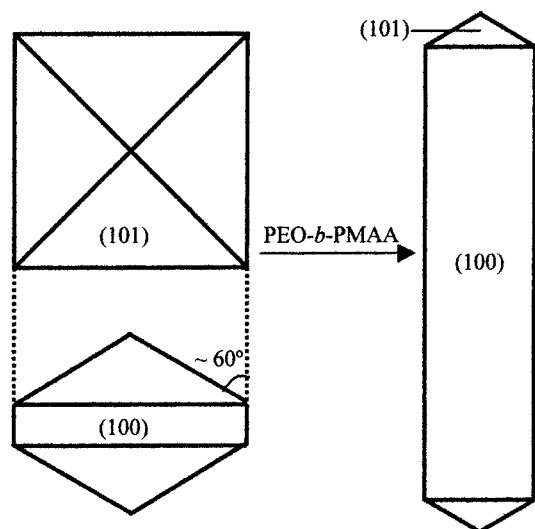
Figure 2. XRD patterns of calcium oxalate crystals obtained in the absence (a) and the presence (b, c) of PEG-*b*-PMAA. [polymer]: (a) 0, (b) 0.2, and (c) 2 g L^{-1}; [CaC$_2$O$_4$] = 1 mM. Peaks characteristic of COT and COD were labeled as "T" and "D", respectively. The indexed peaks were from COD.

COT platelets totally disappeared and the tetragonal COD bipyramids were considerably elongated along the *c*-axis, exhibiting well-developed tetragonal {100} prisms. The square prisms range from 0.6 to 1.2 μm in side length and from 0.3 to 0.6 μm in side width. It is noted that a few twinned or polynucleated COD crystals were present in addition to the well-defined tetragonal prisms with pyramidal endcaps. The corresponding XRD pattern (Figure 2b) shows the appearance of only (200) and (400) peaks of COD, suggesting a preferential alignment of the (100) plane parallel to the specimen surface, which is consistent with the SEM observation that the tetragonal COD prisms generally lay on the {100} planes. It has been documented that increased concentration of additives, such as carboxylic acids[48] and anionic polyelectrolytes,[49] would inhibit the COT phase, resulting in precipitation of the COD phase. However, no morphological change of COD crystals from tetragonal bipyramids to elongated tetragonal prisms has been observed in the presence of the organic additives previously used.

As the concentration of PEG-*b*-PMAA was increased to 2 g L^{-1}, the tetragonal prisms were further elongated along the *c*-axis, resulting in rodlike tetragonal prisms (Figure 1c). It can be observed that the elongated tetragonal prisms were rather uniform with an average side length of 2.2 μm and an average side width of 0.62 μm, which gave an aspect ratio as high as 3.5. Occasionally, twinning of rodlike tetragonal prisms, which resulted in the appearance of "crosses", was also observed. The XRD pattern shown in Figure 2c also reveals largely intensified (200) and (400) peaks of COD, confirming the formation of the rodlike tetragonal prisms dominated by the {100} faces of COD. A schematic representation of the morphological influence of PEG-*b*-PMAA on COD crystals has been shown in Figure 3, which strongly indicates preferential adsorption or specific inhibition of PEG-*b*-PMAA on the {100}

Figure 3. Schematic representation of the morphological influence of PEG-*b*-PMAA on COD crystals. It shows a morphological transition of COD crystals from tetragonal bipyramids dominated by the {101} faces to elongated tetragonal prisms dominated by the {100} faces.

planes of COD crystals. It is noteworthy that such rodlike COD crystals have been found in plants such as *Allium cepa*[54] and *Dracaena sanderiana*.[38] To the best of our knowledge, this is the first time that the rodlike COD crystals exhibiting dominant {100} faces have been prepared in vitro. The present result may have implications for the specific functions of crystal-associated matrix macromolecules in the morphological control of COD crystals in plants.

To gain additional evidence for the formation mechanism of the rodlike COD crystals obtained here, we tried to follow the morphological development of the COD crystals at different crystallization times. However, it was observed that the rodlike crystals formed immediately after the solution became turbid and the products separated within 30 min already showed crystal size and shape similar to the final products. This result indicated that the crystallization of COD crystals was so fast that it was difficult to clearly distinguish between processes occurring during nucleation, growth, and ripening stages at the present time. This observation is reminiscent of the crystallization of calcite in the presence of PEG-*b*-PMAA, where there was also a very fast crystallization process.[32]

Effect of the CaC₂O₄ Concentration. To examine the effect of the CaC_2O_4 concentration on the crystallization, the crystallization experiment was repeated at a polymer concentration of 0.2 g L^{-1} but at lower and higher CaC_2O_4 concentrations. At a lower CaC_2O_4 concentration of 0.5 mM, the product was rodlike COD crystals (Figure 4a), which was evidenced by the corresponding XRD result. These rodlike COD crystals were similar to those obtained at a CaC_2O_4 concentration of 1 mM but at a higher polymer concentration of 2 g L^{-1} (Figure 1c), although the present rodlike crystals seemed to be nonuniform and were much smaller (less than 1.2 μm in length and 0.24 μm in width). On the other hand, at a higher CaC_2O_4 concentration of 4 mM, normal bipyramidal COD crystals were obtained (Figure
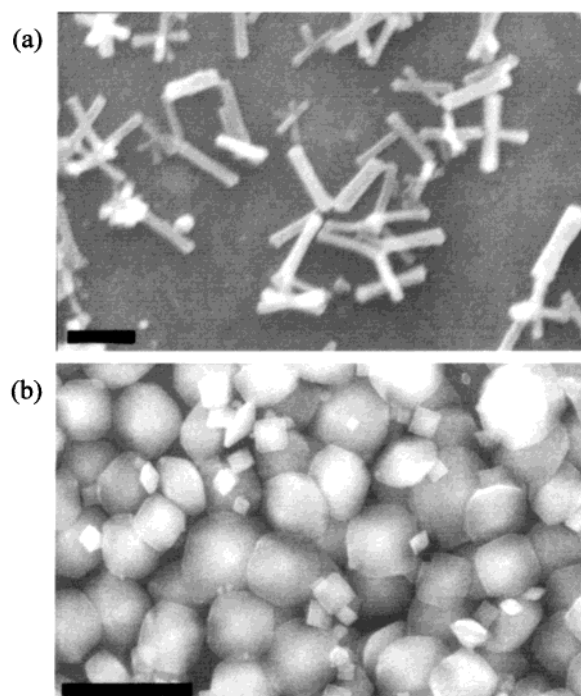
(54) Frey-Wyssling, A. *Am. J. Bot.* **1981**, *68*, 130.

Figure 4. SEM micrographs of COD crystals obtained in the presence of PEG-*b*-PMAA. [polymer] = 0.2 g L^{-1}; [CaC₂O₄]: (a) 0.5 and (b) 4 mM. Scale bars: (a) 1 and (b) 5 μm.

4b). These results suggest that decreasing the CaC_2O_4 concentration at a fixed polymer concentration has a similar effect as increasing the polymer concentration at a fixed CaC_2O_4 concentration. In other words, with decreasing CaC_2O_4 concentration, the adsorption of the polymer on the COD {100} planes was favored, leading to a gradual morphological transition of COD crystals from tetragonal bipyramids dominated by the {101} faces to elongated tetragonal prisms dominated by the {100} faces.

Effect of the [Ca²⁺]/[C₂O₄²⁻] Ratio. Varying the $[Ca^{2+}]/[C_2O_4^{2-}]$ ratio could change the surface electrostatics of COD crystals and thus influence the polymer–COD crystal interaction, leading to a morphological variation of COD crystals. When the polymer concentration was 0.2 g L^{-1} and the oxalate ions concentration was maintained at 1 mM, uniform COD "squares" that exhibit the square prismatic habit with pyramidal endcaps were obtained at a $[Ca^{2+}]/[C_2O_4^{2-}]$ ratio of 1/2 (Figure 5a). The square prisms of the COD squares have an average width of 1.8 μm and an average height of 1.4 μm, resulting in an aspect ratio $\approx$1. Therefore, the {100} planes are less pronounced in these COD squares compared with the elongated tetragonal prisms obtained at the stoichiometric $[Ca^{2+}]/[C_2O_4^{2-}]$ ratio (Figure 1b). This result indicates that the presence of excess oxalate ions at the surfaces of COD crystals could somewhat impair the adsorption of the anionic polymer on the COD {100} planes.

In contrast, *c*-axis elongated COD rods, as indicated by the corresponding XRD result, appeared at a $[Ca^{2+}]/[C_2O_4^{2-}]$ ratio of 2 (Figure 5b). It is worth noting that these COD rods generally exhibit rounded surfaces rather than distinct crystal faces typical of the tetragonal COD prisms, typical of nonspecific or pseudo-specific additive–crystal interaction.[15,22] This result suggests that the presence of excess calcium ions at the surfaces

Figure 5. SEM micrographs of COD crystals obtained in the presence of PEG-*b*-PMAA. [polymer] = 0.2 g L^{-1}; [C$_2$O$_4^{2-}$] = 1 mM; [Ca^{2+}]/[C$_2$O$_4^{2-}$]: (a) 1/2 and (b) 2. Scale bars = 2 μm.

of COD crystals could promote the adsorption of the polymer on COD crystal planes other than the {100} planes, resulting in nonspecific inhibition of the COD crystal faces parallel to the *c*-axis.

Effect of Seed Growth. For seed growth experiments, COD seed crystals, which exhibited tetragonal bipyramidal prisms with relatively uniform size, were prepared in a polymer solution with a [Ca^{2+}]/[C$_2$O$_4^{2-}$] ratio of 1/4. As shown in Figure 6a, the obtained COD seed crystals were basically bipyramids elongated slightly along the tetragonal axis showing side faces about 0.7 μm (along the axis) × 2.7 μm (perpendicular to the axis). As indicated above, a lower [Ca^{2+}]/[C$_2$O$_4^{2-}$] ratio could lead to COD crystals with less pronounced {100} planes possibly because of an impaired interaction of the anionic polymer with the COD {100} planes; therefore, it is reasonable that the present solution condition was favorable for relatively flat bipyramidal prisms.

Seed growth experiments demonstrate that PEG-*b*-PMAA can have a dramatic effect on the COD crystal morphology. The flat bipyramidal prisms were used as seed crystals and were allowed to grow in the solution where COD rods as shown in Figure 1c were obtained in the absence of seed crystals. The produced COD crystals (Figure 6b) consisted of two kinds of crystal morphologies, that is, normal tetragonal rodlike prisms and tetragonal square prisms. Obviously, the relatively small rods corresponded to the crystals nucleated separately whereas the square prisms with a size of 1.7 μm × 2.9 μm resulted from crystal growth on seed crystals of the flat bipyramidal prisms. It was noted that the side length perpendicular to the axis just increased a little (from 2.7 to 2.9 μm), but the side length along the axis increased significantly (from 0.7 to 1.7 μm). This result suggested that PEG-*b*-PMAA can interact strongly with the COD {100} planes, leading to the elongation
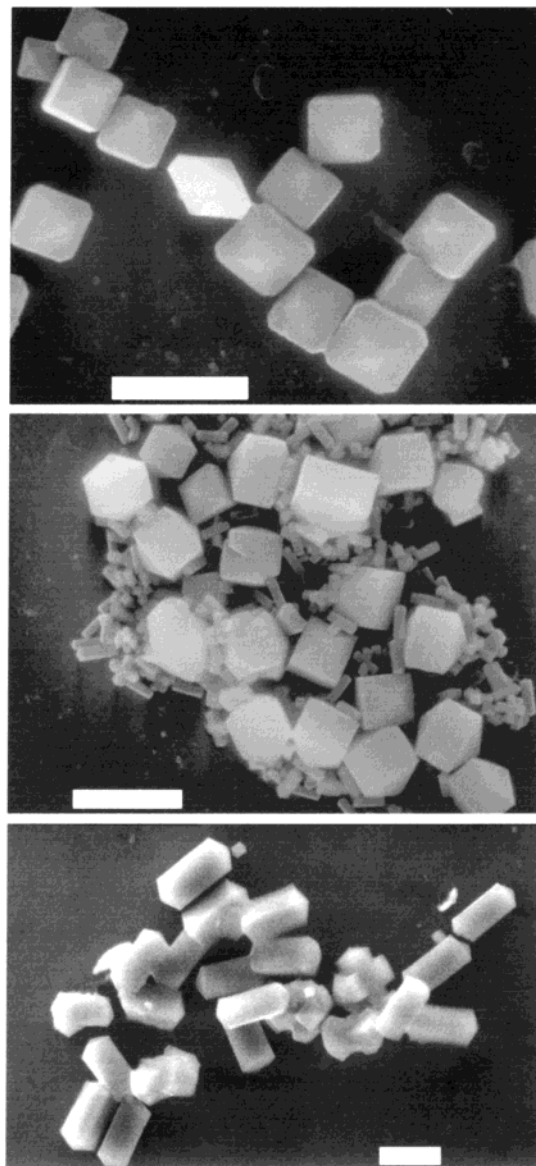

Figure 6. SEM micrographs showing the effect of PEG-*b*-PMAA on the growth of COD seed crystals. (a) Bipyramidal COD crystals obtained in the presence of PEG-*b*-PMAA ([polymer] = 0.2 g L^{-1}; [C$_2$O$_4^{2-}$] = 1 mM; [Ca^{2+}]/[C$_2$O$_4^{2-}$] = 1/4). (b) COD crystals grown from seed crystals of the COD bipyramidal prisms as shown (a) in the solution where COD rods as shown in Figure 1c were obtained in the absence of seed crystals. (c) COD crystals grown from seed crystals of the COD rodlike prisms as shown in Figure 1c in the solution where COD bipyramidal prisms as shown in (a) were obtained in the absence of seed crystals. Scale bars: (a) 5, (b) 5, and (c) 2 μm.

of the flat bipyramidal prisms to exhibit much more pronounced {100} planes.

To further examine the effect of PEG-*b*-PMAA on the COD crystal morphology, the tetragonal rods as shown in Figure 1c were also used as seed crystals and they were allowed to grow in the solution where the flat COD bipyramidal prisms mentioned above were favored. Interestingly, only swollen tetragonal rodlike prisms with a size of 2.3 μm × 1.4 μm were produced (Figure 6c). It can be noted that the side length perpendicular to the axis increased significantly (from 0.62 to 1.4 μm) whereas the side length along the axis just increased a little (from 2.2 to 2.3 μm). This result suggested that

Table 1. Summary of the Experimental Conditions and the Properties of the Calcium Oxalate Crystals Obtained in the Presence of PEG-*b*-PMAA

no.	[polymer] (g L^{-1})	[C$_2$O$_4^{2-}$] (mM)	[Ca^{2+}]/ [C$_2$O$_4^{2-}$]	seed crystals	crystal polymorph	crystal shape	crystal size (μm)^a
1	0	1	1	no	COT, COD	plates, tetragonal bipyramids	>10, 4
2	0.2	1	1	no	COD	tetragonal square prisms	0.6−1.2 × 0.3−0.6
3	2	1	1	no	COD	tetragonal rodlike prisms	2.2 × 0.62
4	0.2	0.5	1	no	COD	tetragonal rodlike prisms	≈1.0 × ≈0.2
5	0.2	4	1	no	COD	tetragonal bipyramids	0.8−4
6	0.2	1	1/2	no	COD	tetragonal square prisms	1.4 × 1.8
7	0.2	1	2	no	COD	rounded rods	0.6−1.8
8	0.2	1	1/4	no	COD	tetragonal bipyramidal prisms	0.7 × 2.7
9	2	1	1	no. 8	COD	tetragonal square prisms	1.7 × 2.9
10	0.2	1	1/4	no. 3	COD	tetragonal rodlike prisms	2.3 × 1.4

^{a} For tetragonal prisms, the crystal size was represented as $m \times n$, where m means the side length along the tetragonal axis and n means the side length perpendicular to the tetragonal axis.

PEG-*b*-PMAA interacted just weakly with the COD {100} planes under this solution condition, leading to the swell of the rodlike prisms to exhibit more pronounced {101} cap faces and just a little more pronounced {100} planes. The crystal properties of the calcium oxalate obtained in the presence of PEG-*b*-PMAA in this work together with the experimental conditions have been summarized in Table 1.

Discussion

Double-hydrophilic block copolymers of the PEG-*b*-PMAA type have been previously used for the morphological control of a variety of inorganic crystals. In most cases, morphologies showing rounded surfaces such as ellipsoids, peanuts or dumbbells, and spheres were obtained, which suggests the presence of nonspecific polymer−crystal interactions.[28−33] A distinct exception was the ZnO system where hexagonal prismatic ZnO crystals grew shorter along their 6-fold screw axis with increasing PEG-*b*-PMAA concentration.[34] It has been proposed that the preferential adsorption of the PMAA block to {001} faces of ZnO would result in shorter hexagonal prismatic crystals; however, the origin of the specific polymer−crystal interaction has not been discussed. Note that the case of ZnO is in good contrast to the present case of calcium oxalate where tetragonal prismatic COD crystals grew longer along their 4-fold axis with increasing PEG-*b*-PMAA concentration.

According to the morphological influence of PEG-*b*-PMAA on COD crystals as shown in Figure 3, it is reasonably deduced that specific interaction between PEG-*b*-PMAA and the COD {100} faces resulted in a gradual morphological transition of COD crystals from tetragonal bipyramids to elongated tetragonal prisms with increasing PEG-*b*-PMAA concentration. To help the understanding of the specific interaction between PEG-*b*-PMAA and the COD {100} faces, the ionic structure of the COD (100) face and the molecular structure of the polymer have to be taken into account.

COD crystallizes in the tetragonal system ($a = 12.371$ Å, $c = 7.357$ Å, space group $I4/m$) and normally crystallizes in the form of a tetragonal bipyramid {101}

associated with a small tetragonal prism {100}.[52,55] The unit cell holds eight molecules of calcium oxalate and consists of alternating water layers and ion layers comprising oxalate and calcium ions, which are oriented parallel to the (100) plane.[56] The polymer PEG-*b*-PMAA used in this work has a structural formula of [PEG]$_{\sim68}$-*b*-[PMAA]$_{\sim6}$,[33] suggesting the PMAA chain is actually rather short with a repeat unit number of about 6. The distance between the neighboring carboxylate groups attached to the PMAA backbone is 2.52 Å, which means that the distance between the first carboxylate group and the sixth carboxylate group would be 12.6 Å whereas the distance between the first carboxylate group and the fourth carboxylate group would be 7.6 Å. Apparently, these two distances match the neighboring calcium ions along the *b*-axis and *c*-axis within the (100) plane of COD crystals, respectively. However, an epitaxial lattice match seems problematic because the polymer backbone may coil and form loops in the solution because of its dynamic nature and thus the actual influence of the polymer would be much more complicated than such a precise lattice matching model. Therefore, we can now only speculate that there exists a possible structural correlation between the short PMAA chain and the COD {100} planes considering that local binding of the polymer must somehow be involved and there will be a preferred mode of polymer adsorption.

To test the proposed mechanism of polymeric additive−crystal interaction, we investigated the crystallization of strontium oxalate in the presence of PEG-*b*-PMAA under similar conditions. It is noted that strontium oxalate forms two hydrates: triclinic SrC$_2$O$_4$·H$_2$O (SOM) and tetragonal SrC$_2$O$_4$·2.5H$_2$O (SOD) that is isomorphic with tetragonal COD with very similar structural parameters, that is, $a = 12.819$ Å, $c = 7.533$ Å, space group $I4/m$.[57] Because a similar structural match exists between PEG-*b*-PMAA and SOD crystals,

(55) Tazzoli, V.; Domeneghetti, C. *Am. Mineral.* **1980**, *65*, 327.
(56) Tunik, L.; Furedi-Milhofer, H.; Garti, N. *Langmuir* **1998**, *14*, 3351.
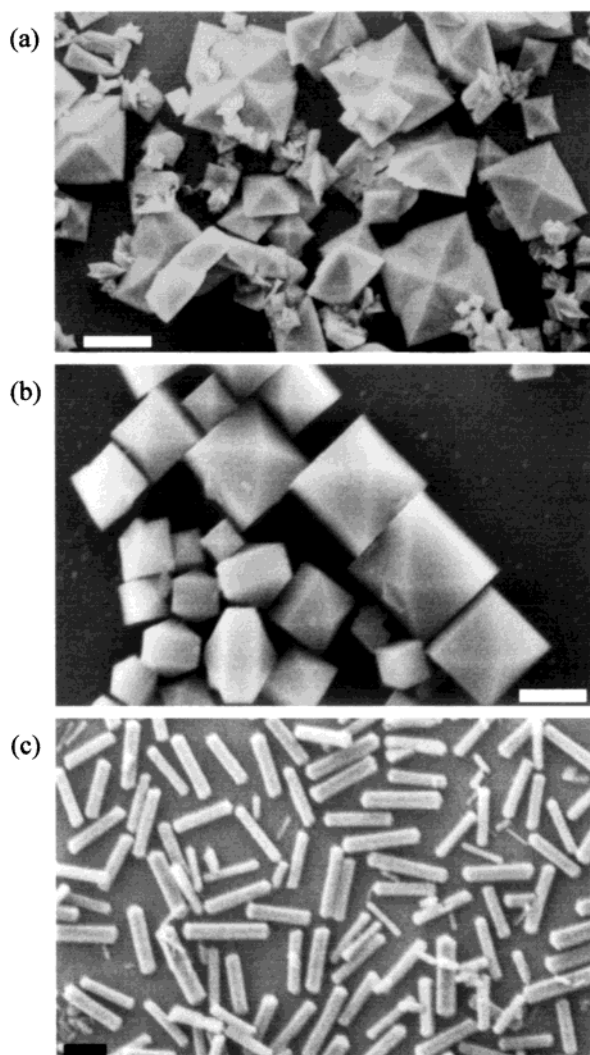(57) Sterling, C. *Nature* **1965**, *20*, 588.

Figure 7. SEM micrographs of strontium oxalate crystals obtained in the absence (a) and in the presence (b, c) of PEG-*b*-PMAA. [polymer]: (a) 0, (b) 0.1, and (c) 1 g L^{-1}; [SrC$_2$O$_4$] = 2 mM. Scale bars: (a) 5, (b) 1, and (c) 1 μm.

it is expected that a similar morphological change of the crystals with increasing polymer concentration would occur. Actually, the experimental result shown in Figure 7 verified this anticipation. It can be seen from Figure 7a that, in the control system where no additives were present, the product was a mixture of aggregated or polynucleated SOM crystals and distorted bipyramids of SOD crystals, the morphology of which is essentially the same as the unstable morphology of COD crystals formed by twist growth.[58] When 0.1 g L^{-1} of PEG-*b*-PMAA was present, the SOM crystals disappeared and the tetragonal SOD bipyramids were slightly elongated along the *c*-axis, exhibiting a small tetragonal {100} prism (Figure 7b). As the concentration of PEG-*b*-PMAA was further increased to 1 g L^{-1}, the short tetragonal SOD prisms were significantly elongated along the *c*-axis, resulting in long tetragonal SOD prisms (Figure 7c), which were very similar to the rodlike tetragonal COD prisms shown in Figure 1c. Therefore, it is indicated that the proposed mechanism of polymeric additive−crystal interaction based on the crystallization of calcium oxalate crystals is possibly applicable to other related systems.

Finally, the unique structural characteristics of PEG-*b*-PMAA, that is, a relatively short binding PMAA block with six repeat units connected to a solvating PEG block, could largely contribute to the specific interaction of the polymer with the {100} planes of COD crystals. It has been reported that, in the presence of homopolymer PMAA with a relatively large molecular weight (M_n = 5000), nonfaceted dumbbells of COD crystals were obtained.[49] Obviously, homopolymer PMAA with a large number of repeat units showed nonspecific interaction with COD crystals, even though the structural fit between PMAA and the COD {100} faces still existed. A possible reason is that a PMAA molecule with a large number of carboxylate groups or binding motifs may simultaneously interact with many crystal faces other than the {100} faces, resulting in nonspecific inhibition to the COD crystal surfaces. On the other hand, the presence of a solvating PEG block could contribute to stabilizing the specific adsorption of the copolymer on the COD {100} faces and prevent possible crystal agglomeration through its steric shielding effect. This may endow the double-block copolymer PEG-*b*-PMAA with considerable advantages in morphological control of COD crystals over low-molecular-weight additives carrying several functional groups capable of interacting specifically with COD crystal surfaces.

Admittedly, the proposed lattice matching model is an extremely simple model and needs to be proved by real evidence, although such a model has been numerously used to explain the interaction between organic templates/additives and inorganic faces.[18,26,59−62] Calculations based on molecular dynamics simulations may provide useful information about the understanding of the interaction between organic templates/additives and inorganic faces and, notably, there have been several attractive reports about molecular recognition on the organic−inorganic interface based on molecular dynamics calculations.[21] However, the application of such molecular modeling techniques still has not been extended from low-molecular-weight additives to polymeric additives. For example, molecular dynamics calculations have been used for the interaction of polymeric additives with calcite surfaces, but the interplay between various competitive effects makes the adsorption process very complex and it is not yet possible to unequivocally relate the chemical structures of the polymers to their different adsorption behavior.[63] This may be the reason the lattice matching model is still most often applied when the interaction between polymeric additives and inorganic surfaces is considered.[26,60,64,65] Nevertheless, it is clear that much effort is required to carry out thorough molecular dynamics calculations to fully elucidate the mechanism of the morphological control of COD crystals by PEG-*b*-PMAA.

(58) Nenow, D.; Vitkov, L. *J. Cryst. Growth* **1997**, *182*, 461.
(59) Litvin, A. L.; Valiyaveettil, S.; Kaplan, D. L.; Mann, S. *Adv. Mater.* **1997**, *9*, 124.
(60) Ueyama, N.; Hosoi, T.; Yamada, Y.; Doi, M.; Okamura, T.; Nakamura, A. *Macromolecules* **1998**, *31*, 7119.
(61) Champ, S.; Dickinson, J. A.; Fallon, P. S.; Heywood, B. R.; Mascal, M. *Angew. Chem., Int. Ed.* **2000**, *39*, 2716.
(62) Davey, R.; Rebello, A. M. M. *Cryst. Growth Des.* **2001**, *1*, 187.
(63) Hadicke, E.; Rieger, J.; Rau, I. U.; Boeckh, D. *Phys. Chem. Chem. Phys.* **1999**, *1*, 3891.
(64) Naka, K.; Chujo, Y. *Chem. Mater.* **2001**, *13*, 3245.
(65) Estroff, L. A.; Hamilton, A. D. *Chem. Mater.* **2001**, *13*, 3227.

In conclusion, it has been demonstrated that the presence of PEG-*b*-PMAA generally favors the morphological transition of COD crystals from tetragonal bipyramids dominated by the {101} faces to elongated tetragonal prisms dominated by the {100} faces. It is speculated that the structural correlation between the short PMAA chain and the COD {100} planes could be responsible for the specific interaction between them, which resulted in the observed morphological control of COD crystals by PEG-*b*-PMAA. The observed morphological control of COD crystals by the polymeric additive provides insights into the specific function of biomacromolecules in the morphological control of plant COD crystals and could be applied to other synthetic systems of interest.

CM010768Y